

CHAPTER 11

Ship design and offshore engineering require not only estimates of wave height h_{max} but also information on wave frequency spectrum $S(\omega)$ that corresponds to extreme wave conditions. Recent years have been marked by the availability of new wave observations. Automated buoys started to measure waves regularly in the offshore waters of many countries [Hamsley, 1996].

Wave measurements from satellites now cover a period of almost 15 years. The wave data exists as measured and simulated wave heights and wave spectra, both omni-directional $S(\omega)$ and directional $S(\omega, \beta)$. They are functions of spatial co-ordinates (such as x, y) and time t . Thus, it is possible to draw some parallel between a "wave weather ensemble" and a wave spectra $S(\omega, \beta, x, y, t)$ ensemble, and to make a step from classification of wave heights to a classification of spectra. The term «spectral wave climate» was approved by a major conference on wind waves (1998), in which experts representing open ocean shipping, shelf engineering and construction participated along with specialists in wave modelling and research ["Provision ...", 1998].

Let us consider several examples of wind wave spectrum variations during a storm passage.

Fig. 11.1 shows an example of the variation of the frequency spectrum $S(\omega, t)$ at a point located in the North Atlantic, as measured by RV "Weather Reporter" of the UK, from 15th to 19th December 1959 [Wilson, 1965]. The upper panel of the figure also shows data on wind speed u , wave height variance D_{ζ} , and mean wave period τ . Wind strengthening up to 30 knots occurred from 6 to 18 h December 16, 1959. The wind wave spectrum during that period of time did not change significantly. From 18 h December 16th to 03 h December 17th the wind veered and strengthened up to 62 knots.

The wave spectrum was growing quickly and reached its peak by 18 h December 17. Then, it weakened a little following a corresponding decrease in the wind speed and again strengthened reaching the maximum at 0 h December 18th. Subsequent variations of the spectrum correspond to the storm wave decay.

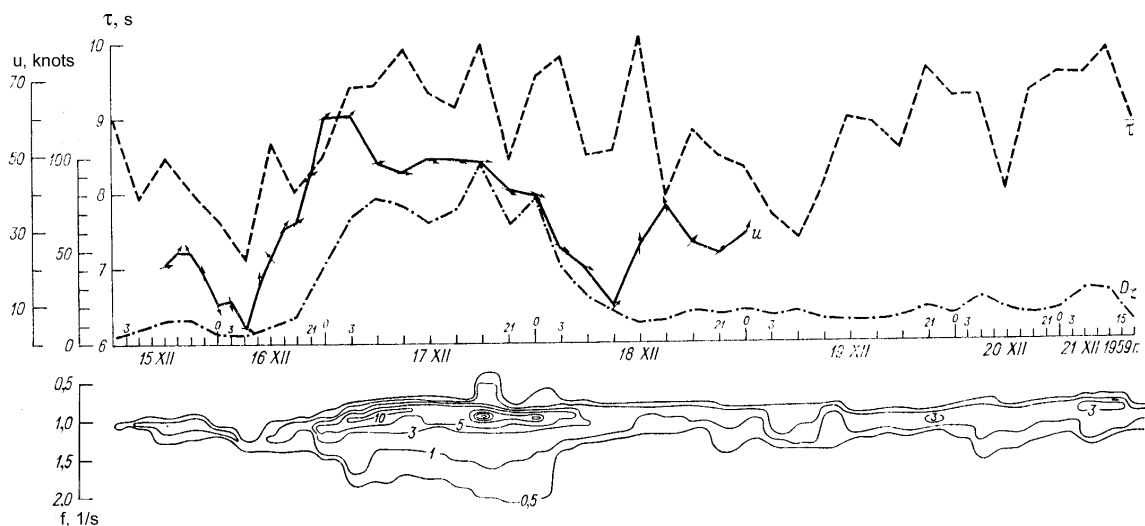


Figure 11.1: Lower panel: An example of variations of frequency spectrum $S_{\zeta}(\omega, t)$ ($m^2 \cdot s$). The upper panel: variations of total variance $D_{\zeta}(t)$ (m^2), mean wave period τ (s) and wind speed u (knots).

Fig. 11.2 shows sections of function $S(\omega, t)$ from 22nd August to 6th September 1966 measured by research vessels "Iceberg" of Russia and "Weather Adviser" of the UK. Three phases of storm development can be noticed, namely a development of wind sea from an initial complex wave field, then a transformation of the wind wave to swell and, finally, the existence of a new complex wave field.

From August 28 to September 6, 1966, Ocean Weather Station (OWS) "1" experienced the impact of three cyclones and the hurricane "Vera". Features of the wind wave spectrum variations that were observable by naked eye were its growth under the action of a strengthening wind and associated changes of the total spectrum variance. Then, following a change of wind direction, the wave field became mixed, and the spectrum

developed a second peak. The storm decay was accompanied by a decrease of the total wave spectrum variance. Later on, swell started to dominate the whole pattern. These processes are seen in Fig. 1.3.

According to [Goldman, 1977], it is possible to reconstruct conditions of a hypothetical (artificial) storm that would lead to the highest practically possible waves at a location of interest. The idea is to look at a situation that did not happen as yet but can, in principle, happen in future.

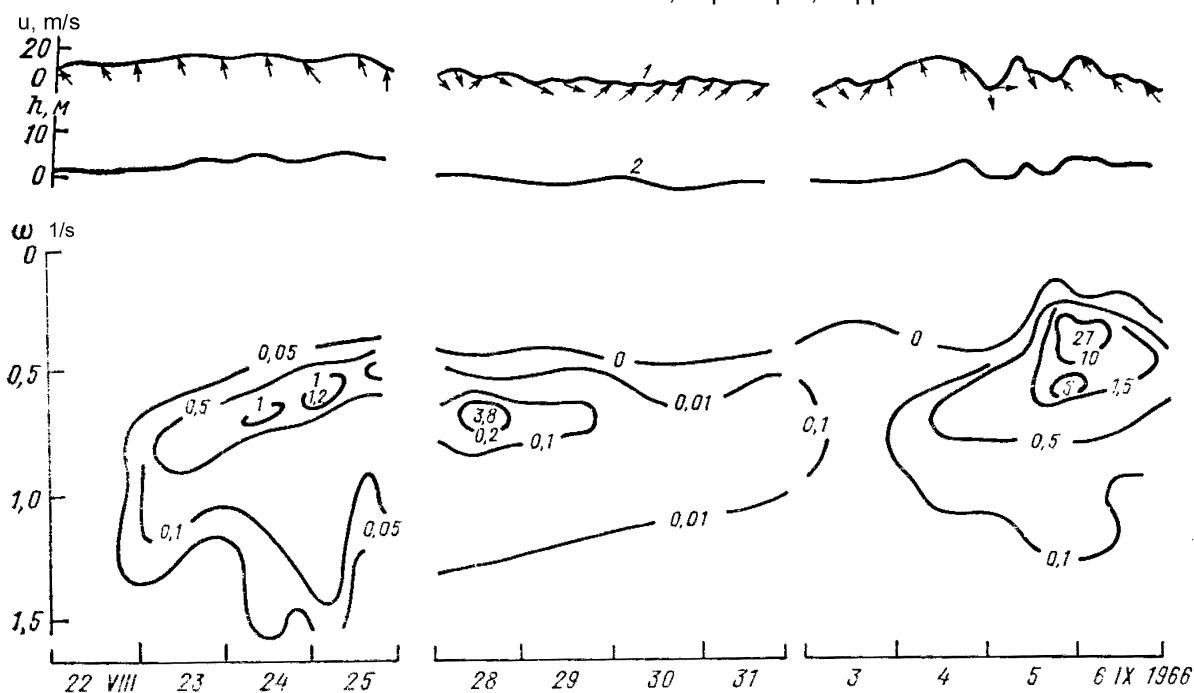


Figure 11.2: Spectral density $S(\omega, t)$ ($m^2 s$) of wind waves in the North Atlantic from August 22 to September 6, 1966. 1: wind speed (m/s), with arrows indicating the direction. 2: significant wave height (m).

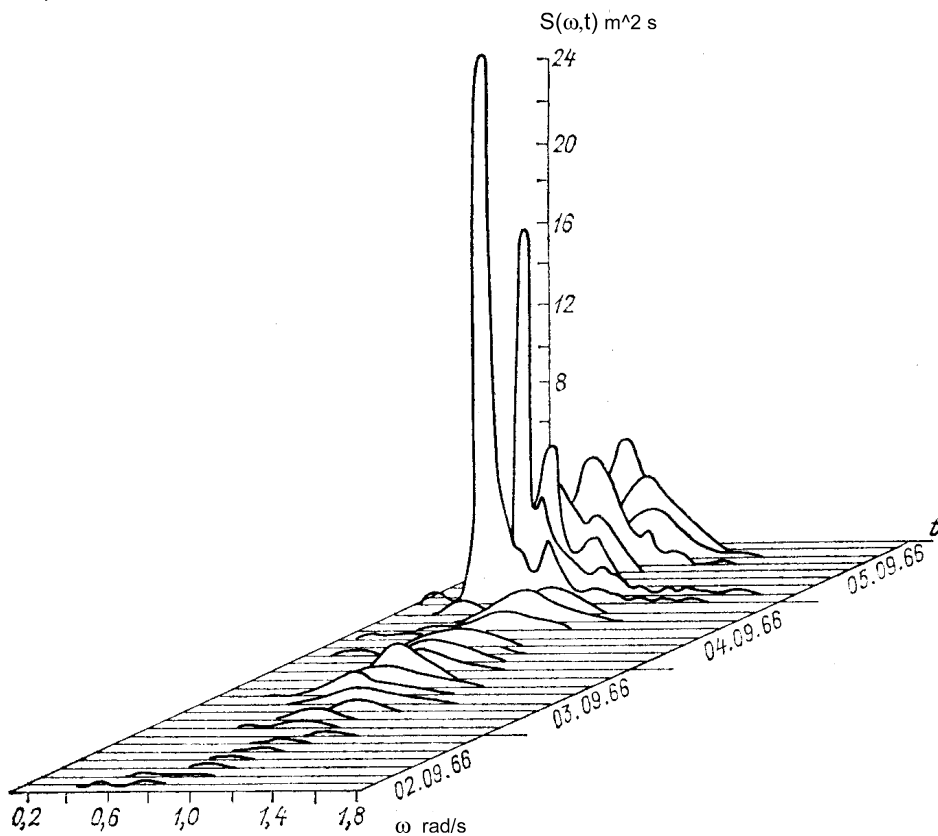


Figure 11.3: Changes of wave frequency spectrum at OWS "I" during the hurricane "Vera".

For example, for the Gulf of Alaska, and for area around Iceland, a combined wave height of 35 m could be anticipated. The combined wave was composed of a wind wave (sea) of 33 m with period of 27 s, and a swell wave of 12 m with period of 31 s. It was generated in conditions of strong atmospheric pressure gradients along a cold front. Persistent strong winds blew over fetches of several hundreds of kilometers superimposed on considerable horizontal gradients of sea surface temperature. Apparently, the geographical and meteorological conditions of both areas do not preclude such a combination of factors from happening. However, the possibility that such storm could happen requires additional study.

Participants at the 18th Assembly of the International Maritime Organization (1993) agreed upon the following definition. The extreme wave spectrum is to be understood as the spectrum corresponding to the maximal possible value of significant wave height (h_s) derived using wave measurements at different locations during time period not shorter than 10 years. The climatic wave spectrum is defined as the averaged spectrum over an ensemble of spectra that have a certain probability, and correspond to dominant

$$S(\omega) = \frac{1}{4} \sum \frac{[\omega_{m_j}^4 (4\lambda_j + 1)/4]^{k_j}}{\Gamma(\lambda_j)} \frac{(h_s^2)_j}{\omega^{4\lambda_j+1}} \exp\left[-\frac{4\lambda_j + 1}{4} \left(\frac{\omega_{m_j}}{\omega}\right)^4\right] \quad (11.2)$$

where h_s denoted significant wave height, ω_m was the frequency of the spectral maximum, λ was a parameter defining shape of the spectrum, and $\Gamma(\lambda)$ was the Gamma-function.

Equation (11.2) takes into account that, as a rule, wave spectra contain two peaks, at low and higher frequencies. This makes it possible to find a correspondence between a series of spectra $S_i(\omega)$, $i=1, \dots, n$, and six parameters $(h_s, \omega_m, \lambda)_j$, $j = 1, 2$. Then these parameters can be used in developing a classification of wind waves.

[Buckley, 1988] analyzed more than 2 million spectra that were generated over 12 years at 13 buoys located in coastal waters of the USA. All the wave situations that the study included were broken down into twelve types, according to their significant wave height. The highest waves had $h_s > 9.5$ m. The abundance of data series made it possible not only to compute the average spectrum $\bar{S}(\omega)$ for all the classes, but even to derive a distribution function $F_s(x)$ and corresponding quantiles $S_p(\omega)$ of this distribution. Fig. 11.4 gives three statistical characteristics of spectra corresponding to two classes of h_s .

It is relevant to note that the quantile spectrum $S_p(\omega)$ for given probability p , e.g. for $p = 0.05$,

wave generation conditions over the area. Some progress in studying the climatic wave spectra can be reported.

The first averaged wave spectra were computed using 204 wave records at OWS "I" in the North Atlantic. Wind speeds there ranged between 2 and 25 m/s and mean wave heights varied from 0.5 to 4.5 m [Skott, 1968].

The following approximation was obtained for the average spectrum $\bar{S}(\omega)$:

$$\bar{S}(\omega, h_s, \bar{\tau}) = \left(\frac{h_s}{3.98}\right)^2 \bar{\omega}^4 \omega^{-5} \exp\left[-0.318 \left(\frac{\bar{\omega}}{\omega}\right)^4\right] \quad (11.1)$$

Relation (11.1) makes it possible to compute $\bar{S}(\omega)$ for some areas of the World Oceans and for different seasons, provided two-dimensional (height and period) distributions are known (e.g., from a reference book).

[Ochi, 1978] analyzed 800 spectra of wind waves at nine Ocean Weather Stations in the North Atlantic, and showed that the most general representation for such spectra would be

coincides for every frequency ω_k with different spectra $S_i(\omega_k)$. Thus, $S_{max}(\omega_k)$ is the upper envelope for the family of spectra $S_i(\omega_k)$ composed of maximum elements in samples (S_1, \dots, S_n) composed of values $S_i(\omega_k)$ for $i=1, \dots, n$ (where n is number of spectra in the sample). Only tuning of the parameters can force the spectrum $\bar{S}(\omega)$ to coincide with any known single-peaked or double-peaked approximation, such as (11.1), (11.2) or JONSWAP. Computations of climatic wave spectra for the Barents and Black Seas were carried out in [Lopatoukhin, Boukhanovsky, 1997; Boukhanovsky, Lopatoukhin, Rozhkov, 1998a, Lopatoukhin, et al., 1999].

Several researchers, e.g. [Vincent et al., 1977], represent ensemble $S_i(\omega_k)$ using the expansion with respect to orthogonal eigen-components:

$$S_i(\omega_k) = \sum_v a_{iv} \varphi_v(\omega_k) \quad (11.3)$$

where $\varphi_v(\omega_k)$ denote basis functions and a_{iv} are coefficients.

The fastest convergence of series (11.3) takes place when $\varphi_v(\omega_k)$ are equal to eigenfunctions of the correlation matrix $K_{S^*}(\omega_i, \omega_j)$ of spectral estimate $S^*_i(\omega_k)$.

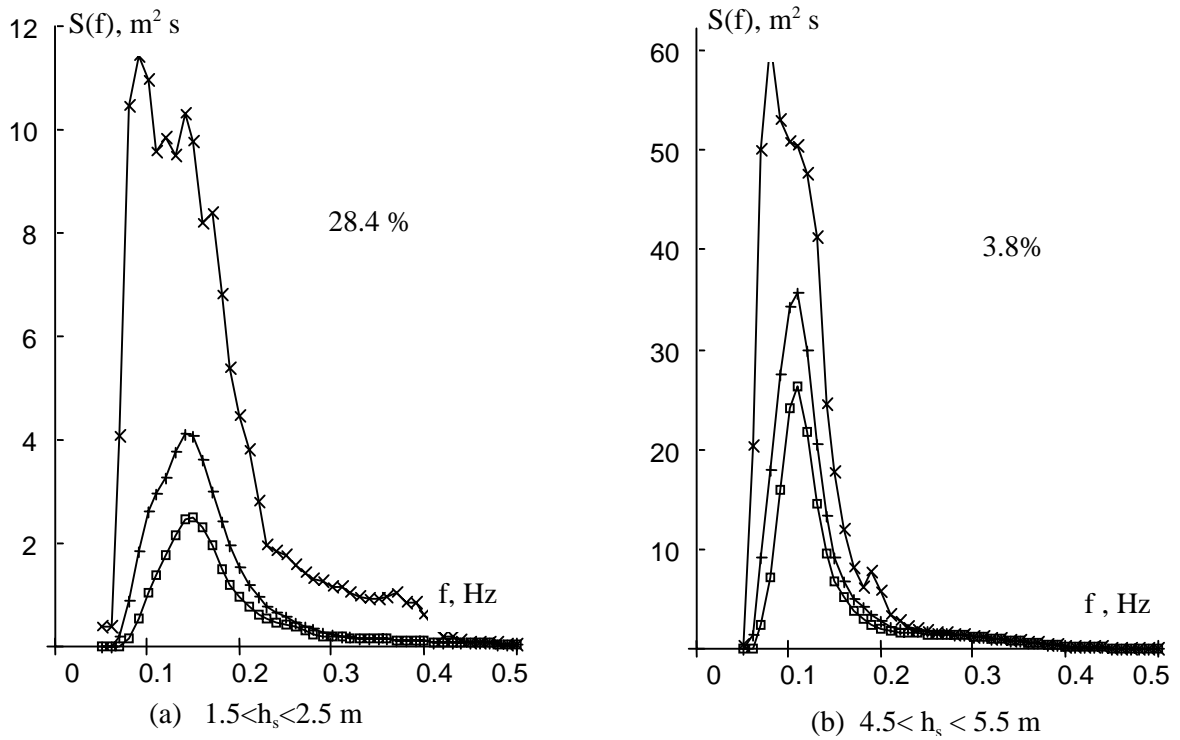


Figure 11.4: Climatic wave spectra for buoy No. 44004 (Atlantic coast of the USA) [Buckley, 1988], (a): sample of 8771 spectra, (b): sample of 1156 spectra. Notations: —□— denotes mean spectrum, —+— stands for the mean spectrum plus standard deviation, and —x— denotes the maximal spectrum. Values of 28.4% and 3.8% are the probability of spectra in this location

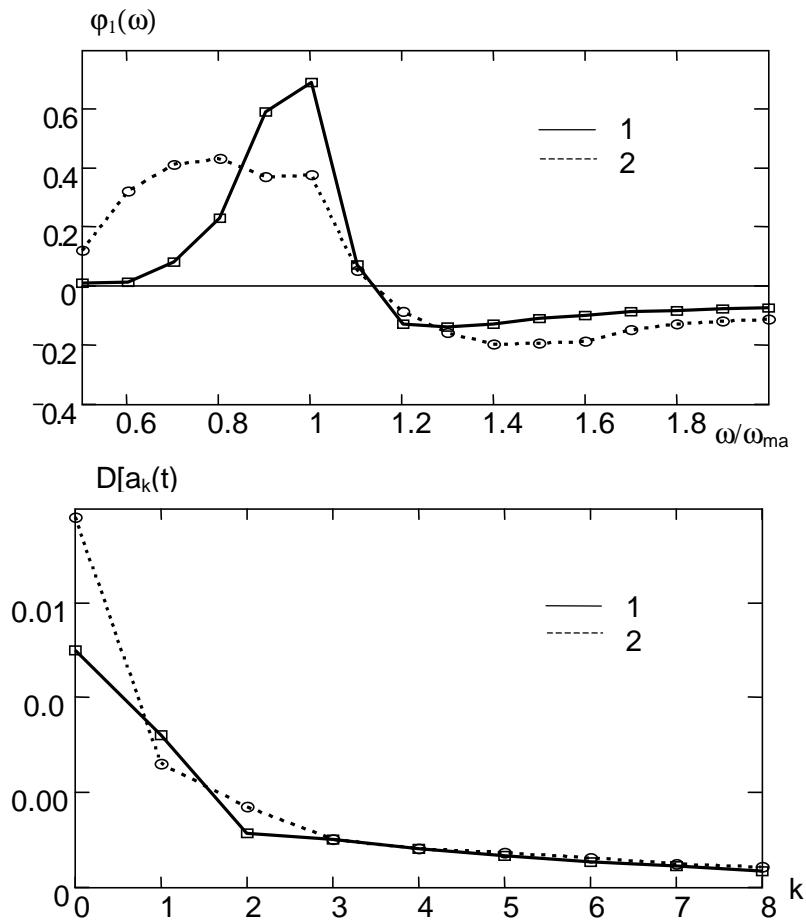


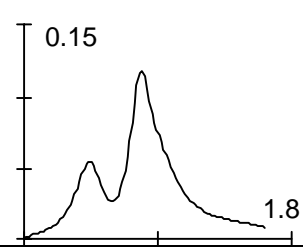
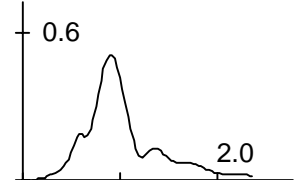
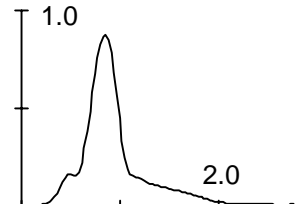
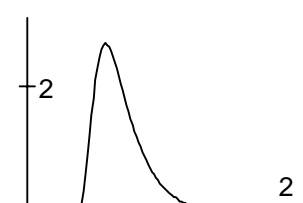
Figure 11.5: First eigenfunctions $\phi_1(\nu)$ and variances $D[a_k]$ of expansion (11.3) for wind wave spectra. 1: wind sea spectra, 2: double-peaked spectra of combined wave field

Fig. 11.5 gives estimates for $\varphi(\omega)$ and variances D_{a_v} of coefficients a_{iv} , which were computed using two kinds of spectra, namely single-peaked spectra of wind waves and double-peaked spectra for mixed waves. These two kinds of spectra differ considerably, but their first eigenfunctions $\varphi_1(\omega)$ are not that different (eigenfunctions $\varphi_v(\omega)$ of higher order being less similar). Variances D_{a_v} decrease rapidly as number v increases.

A classification of spectra $S_i(\omega, h_s)$ based on a single parameter, h_s or dispersion D_ξ , would lead to difficulties in interpretation of probabilistic characteristics. A more fruitful approach, which also leads to a better interpretation of results, is

based on classification with respect to "persistent conditions". For example, [Lopatoukhin et al., 1990] proposed four types of wave generating conditions for the tropical Pacific, leading to development of common features in their spectra (see Table 11.1). Variability of wind wave spectra within each of the four groups can be expressed using quantile diagrams as shown in Fig. 11.6. As can be seen, the main spectral peak $S_{max}(\omega)$ at frequency $\omega_{max} = 0.9$ rad/s can vary from minimal value of $0.4 \text{ m}^2\text{s}$ to a maximum value of $1.2 \text{ m}^2\text{s}$ (with median value of $0.9 \text{ m}^2\text{s}$). ω_{max} varies from 0.6 to 1.0 rad/s. The secondary maximum at $\omega = 0.5$ rad/s, which corresponds to swell, can be as large as $S(\omega) = 0.5 \text{ m}^2\text{s}$, and its frequency can vary in the range of $\omega \in [0.4; 0.6]$ rad/s.

Table 11.1
Typical frequency spectra for the tropical part of the North Pacific Ocean

Type	%	Wind, m/s	Variance, cm^2	Peak No.1, Rad/s	Peak No.2, Rad/s	Spectral shape $S(\omega)$, ($\text{m}^2 \text{ s}$)
ITCZ	40	<6	650-1300	0.4-0.7	0.8-1.1	
MTW	25	<8	1500-2800	0.4-0.7	0.8-1.1	
STW	25	8-15	2500-4500	0.4-0.7	0.7-1.0	
TC	10	>15	>4500	0.4-0.7	—	

Note: ITCZ is Inter-Tropical Convergence Zone, MTW is moderate Trade Winds, STW is strong Trade Winds, TC is tropical cyclone.

[Lopatoukhin, Boukhanovsky et al., 1999] used long term wave measurements in the Black Sea and proposed a classification of wave spectra according to their genesis, i.e. for wind sea, swell

and combined waves (see Table 11.2). They also determined probabilities of their occurrence and of consequential transformations between the different types.

Table 11.2
Probability of wave types

Wave	Subtype	Type	N	Winter	Transient seasons	Summer	Year
Swell	Steep	I-1	366	5%	2%	10%	6%
	Middle	I-2	1037	22%	8%	19%	17%
	Slope	I-3	1220	–	32%	30%	20%
Wind waves		II	1952	47%	27%	22%	32%
Combination without separation	Swell	III-1	793	16%	15%	8%	13%
	Wind waves	III-2	184	4%	4%	2%	3%
Combination with separation	Swell	IV-1	427	5%	10%	7%	7%
	Wind waves	IV-2	123	1%	2%	2%	2%
Total			6102	100%	100%	100%	100%

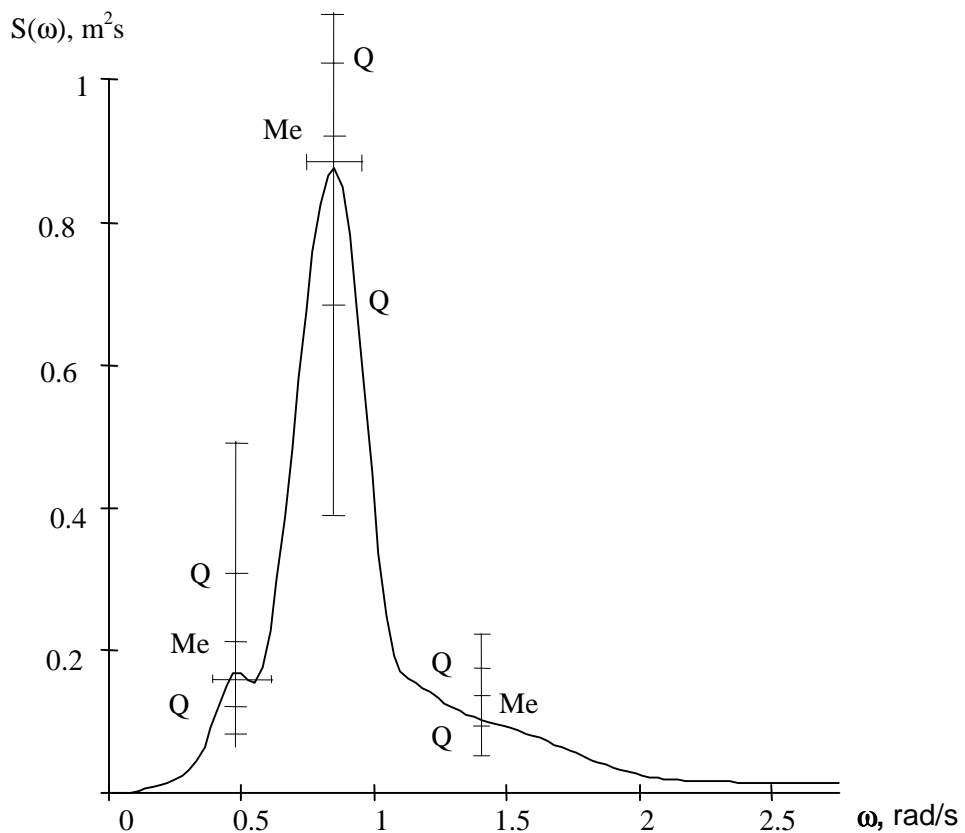


Figure 11.6: A typical wave spectrum generated under the action of strong trade winds in tropical part of the North Pacific Ocean.

Functional representation of such classes of spectral densities $S(\omega)$ can be made using the following well known approximation:

$$S(\omega) = A\omega^{-k} \exp[-B\omega^{-n}] \quad (11.4)$$

where A, B, k, n are parameters reflecting wave generating conditions.

Mean wave height \bar{h} is the only parameter needed for description of the wind sea. Mean wave

period can be estimated by various relations [Wind, 1974], (e.g. as in the chapter 10). A single-peaked spectral approximation (10.4) for swell depends on two parameters, namely \bar{h} and $\bar{\tau}$.

The combination $\delta = g\tau^2/h$ reflects the non-dimensional steepness. A complex wave can be expressed, in the first approximation, as the sum of spectra:

$$S_{Complex}(\omega) = S_{WindSea}(\omega) + S_{Swell}(\omega) \quad (11.5)$$

The proposed approximation uses spectral moments and some other related variables. It makes it possible to represent any spectral density function $S(\omega)$ as $S(\omega, \Xi)$, where Ξ denotes a set of parameters. All operations with such functions $S(\omega)$ inside their class are ones with deterministic functions (11.1), (11.2) or (11.4) of random arguments Ξ . For example it is possible to define the mean spectrum

$$\bar{S}(\omega) = S(\omega, \bar{\Xi}), \quad (11.6)$$

quantile spectrum

$$S_p(\omega) = S(\omega, \Xi_p), \quad (11.7)$$

and variance of spectra:

$$D_S(\omega) \equiv \sum_{i=1}^n \left(\frac{\partial S(\omega)}{\partial \xi_i} \right)_{\xi=\bar{\xi}}^2 D_{\xi_i} + 2 \sum_{i>j} \left(\frac{\partial S(\omega)}{\partial \xi_i} \right)_{\xi=\bar{\xi}} \left(\frac{\partial S(\omega)}{\partial \xi_j} \right)_{\xi=\bar{\xi}} cov(\xi_i, \xi_j) \quad (11.8)$$

In the above expressions $\bar{\Xi}$, Ξ_p stand for sets of mean values of parameters and their quantiles, $D_{\xi_i}, cov(\xi_i, \xi_j)$ are the variance and covariance of the parameters, respectively.

directional spectra $S(\omega, \theta)$ as well. This information is very important in actual applications. [Krogstad et al., 1997; Krogstad, 1998] studied existing approximations for angular wave energy distribution and proposed their generalization.

The above examples dealt with wave frequency spectra only. As mentioned at the beginning of this chapter, a considerable volume of measured and simulated data is available at present not only for omni-directional spectra $S(\omega)$, but for the

The 3-D pattern of a wave spectrum is particularly complicated for moderate wave heights. In the case of a strong storm or "dead" swell the spectrum is characterized by relatively narrow directional distribution.

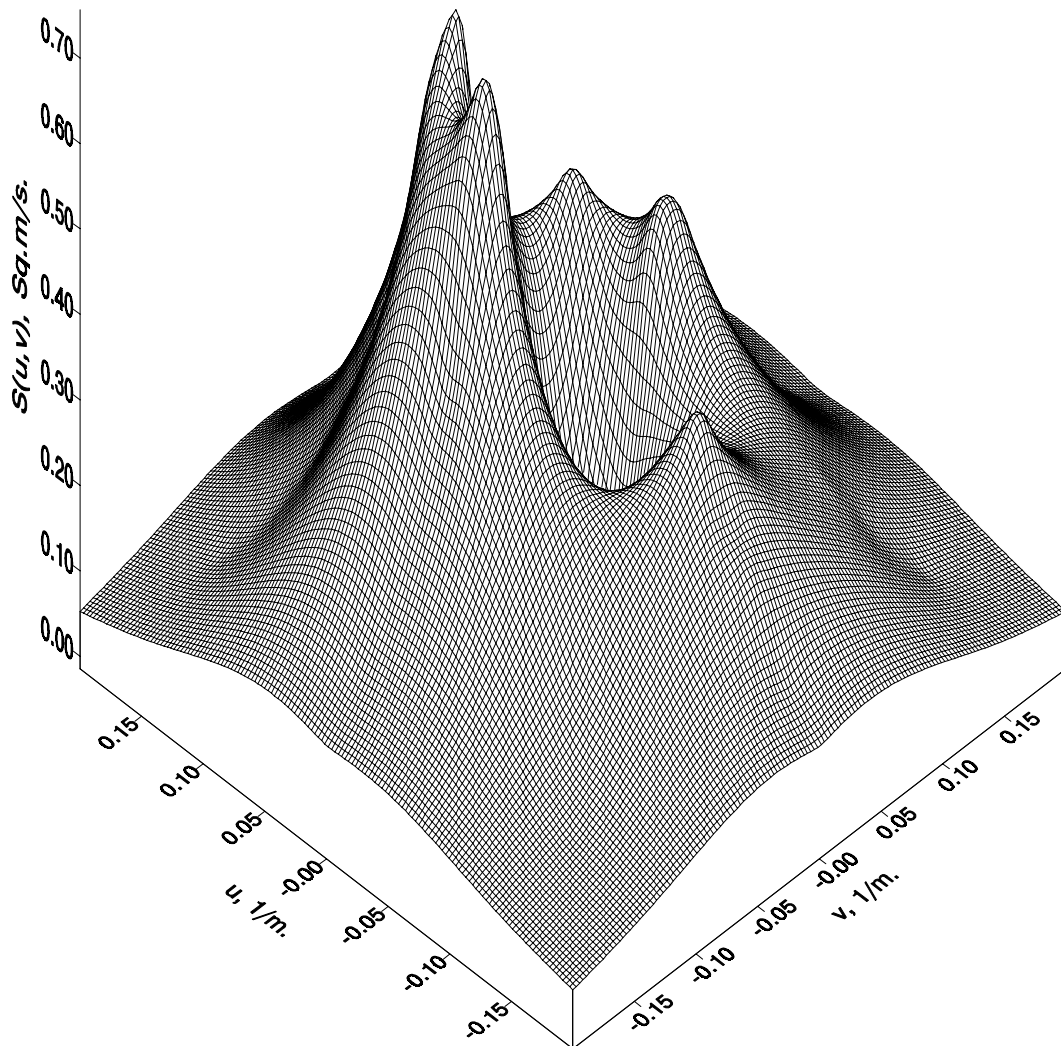


Figure 11.7: Climatic directional spectrum of wave energy for storm conditions in the Barents Sea. It corresponds to 90%- distribution probability of directional spectra

Fig. 11.7 shows a climatic spectrum for storm waves in the Barents Sea. It corresponds to 90% decile of directional wave energy spectra. Further

studies of directional spectra of different intensities are needed.

---oooOooo---